# Mutual Decentralized Synchronization for Intervehicle Communications

Essam Sourour and Masao Nakagawa, *Member, IEEE*

***Abstract*— Data exchange among vehicles can improve road safety and capacity. Most of the proposed intervehicle data communication systems require intervehicle synchronization. Synchronization must be done in a decentralized manner. In this paper, we propose a new mutual decentralized synchronization system. Using a devoted carrier frequency, each vehicle transmits a continuous periodic train of pulses. The aim of the synchronization system is to make these periodic pulses synchronous to indicate the start of data slots in slotted ALOHA types of media access protocol. Each vehicle measures the power of pulses of other vehicles as well as the time difference between other pulses and its own pulse. Using this information, each vehicle shifts its own pulse transmission time toward a weighted average of other pulse transmission times. Eventually, all periodic pulse trains are synchronized. The system performance is evaluated in nonfading and fading channels.**

## I. Introduction

INTERVECHICLE communication plays an important role in the intelligent vehicle highway system (IVHS) [4], [7], [13], [14], [17]–[19]. By exchanging driving intentions among vehicles, intelligent control of speed, acceleration, and headway are achieved. Driving maneuvers such as lane changing, road exiting, and entering become safer and smoother. Quick warning is possible in case of hard braking or accidents. These features add to the safety and capacity of the highway system.

Two main communication systems have been under investigation lately. In the first, optical laser or infrared communication is proposed [9], [11], [12]. In this system, each vehicle can communicate physically with two vehicles only, one in the front and one in the back on the same lane. Information can still flow among all vehicles in data packets stored and forwarded from one vehicle to the other without requiring clock synchronization among vehicles [14]. However, this system is sensitive to transmitter–receiver alignment and weather conditions such as snow, rain, and fog. Also, due to data forwarding, a very low probability of error is required at each receiver for a data packet to reach its destination correctly. Moreover, the delay encountered due to data storing and forwarding can have a negative impact on safety.

The other system, such as the one proposed in the PROMETHEUS program in Europe, utilizes millimeter wave radio frequency (RF) communication [4], [7], [8], [10], [16]. A vehicle broadcasts its information to all vehicles in all directions. If communication in one lane is desirable, a high degree of antenna directivity is possible at this frequency. But pinpoint antenna alignment is not necessary. Reservation ALOHA (R-ALOHA) is widely proposed as the media access protocol for this system, with modifications to meet the vehicle-to-vehicle communication environment [7], [8], [10], [15]. The aim of this paper is to design and evaluate a synchronization technique for this or similar systems.

The scope of the paper does not cover the media access part. However, we assume the following features. All vehicles use the same carrier frequency in a packet communication mode. The channel is structured in time slots of fixed length, which is equal to the data packet length. Since vehicles always have data packets to transmit, each vehicle broadcasts its data periodically on a time slot, with a period common to all vehicles. A vehicle joining the system for the first time must sense the channel and select an idle time slot and transmit (reserve) in this time slot starting from the next period.

Obviously, all vehicles must have a common clock, defining the start of time slots. Since in packet communications a guard time is usually provided, perfect slot synchronization is not necessary. For example, the IS-54 cellular system, with centralized synchronization, sets a guard time between uplink slots that is approximately 2% of the slot duration. For the global system for mobile communication (GSM) system with a higher data rate, this number is about 5%. The vehicle-to-vehicle communication system proposed in [7] assumes a guard time between slots that is 20% of the slot period. Therefore, the goal of the proposed synchronization system is to establish a common clock for all vehicles for slot synchronization with an acceptable error. The guard time is also necessary to allow for clock jitter in the transmitters and receivers.

Despite the large volume of research in the area of vehicle-to-vehicle communication, very little work is available in the literature regarding the synchronization part of the system. In [6], a synchronization technique is proposed. Each vehicle counts the number of other vehicles synchronized with itself, and transmits that weight on its data packets. A new vehicle synchronizes to the vehicles with highest weight. This technique requires new vehicles to be able to detect data packets before they are synchronized. In [4], Valade describes an experimental prototype for PROMETHEUS and states that synchronization is obtained by a recursive convergence toward a weighted average of the slot times of received vehicles during previous cycles. No more details were provided in [4].

Manuscript received June 27, 1996; revised November 12, 1998.

E. Sourour is with Ericsson, Inc., Research Triangle Park, NC 27709 USA.

M. Nakagawa is with the Department of Electrical Engineering, Keio University, Yokohama-shi, Kanagawa 223-8522, Japan (e-mail: nakagawa@nkgw.ics.keio.ac.jp).

Publisher Item Identifier S 0018-9545(99)09129-X.

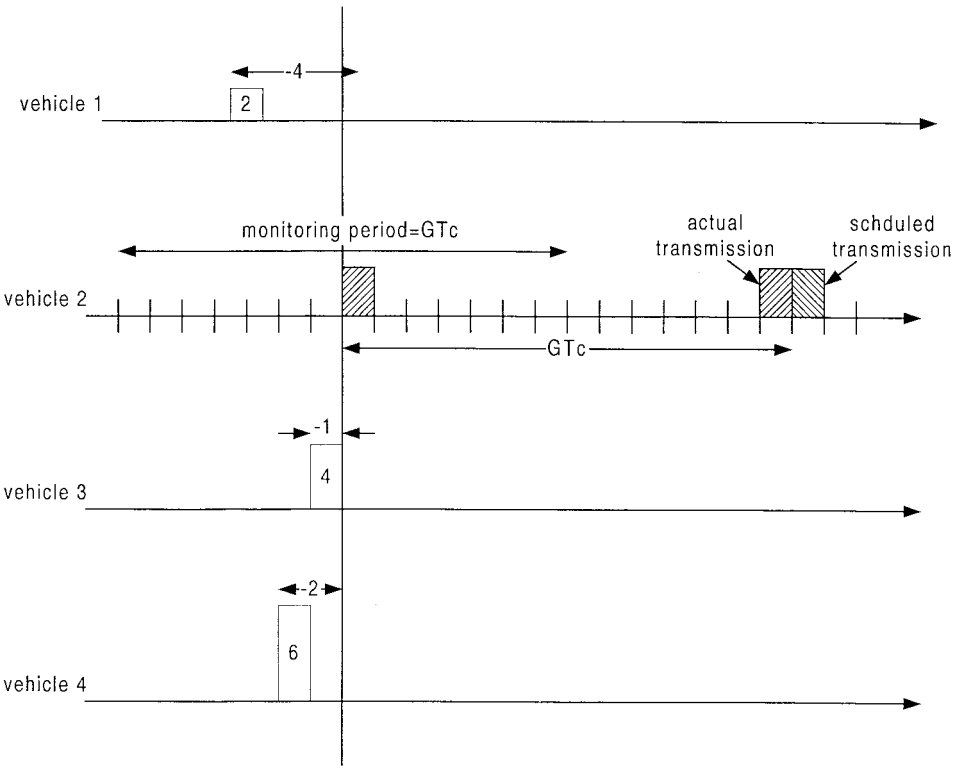


Fig. 1. One iteration for vehicle 2 applying (1) with $\alpha = 0.5$. Numbers inside pulses indicate power measured by vehicle 2.

This method appears to be the one originally proposed by Akaiwa *et al.* in [1] for decentralized interbase station synchronization in microcellular systems. Akaiwa's method was the basis of many proposals for decentralized synchronization in microcellular systems [2], [3] and a proposal for intervehicle synchronization [5].

Our proposed decentralized synchronization technique also depends on Akaiwa's method. We design a system that takes into consideration the vehicle-to-vehicle environment where the number of vehicles is unknown. Also, due to the absence of central coordination, all vehicles must use the same carrier frequency for intervehicle synchronization. Briefly, our method is as follows. One carrier frequency is continuously devoted for synchronization. Each vehicle continuously transmits periodic pulses with a period equal to the data slot length. Data communication is done in parallel on a separate frequency, which we are not concerned about in this paper. Each vehicle measures the power due to these pulses, during one period that is centered by its own pulse transmission time. Also, during the same period, each vehicle measures the delay of the detected pulses, with respect to (w.r.t.) its own pulse transmission time. Each vehicle calculates a power-weighted average of these delays. The next pulse transmission time, which is supposed to be after one period, is advanced or retarded by this value. It is worth noting that, due to the single frequency utilization, a vehicle does not monitor the channel at the instance when it transmits a pulse. This has a small effect on the synchronization process as shown later. This method is studied in nonfading and fading channels using computer simulation.

The paper is organized as follows. Section II presents the synchronization technique. Section III introduces the channel model used in the paper. Section IV analyzes the envelope detector output due to the synchronization signals, taking into account the channel model. Section V describes the simulation procedure, while Section VI presents the numerical results. The last section is devoted for the findings and conclusions.

## II. Mutual Decentralized Synchronization

In [1], Akaiwa *et al.* proposed a recursive formula for autonomous decentralized synchronization for microcellular system base stations. For a number of stations to get synchronized over the air, each station is required to measure the power and the delay offset (positive or negative) of other stations w.r.t. its own signal. Exact measurement of power is sometimes not necessary, and synchronization can be achieved, at some conditions even faster [2], using on–off decision about existence of received signal power. Knowledge of the propagation delay among neighboring stations can also be used in Akaiwa's formula. If propagation delay is not used, base stations can still synchronize, but with a clock drift. In a microcellular environment the base stations within power reach of each other are assigned different frequencies, and, hence, measurement of power and relative delay is easily achievable [1]–[3]. Moreover, since the physical locations are known in advance, the propagation delay is also known. On the other hand, in intervehicle communication environment the latter two assumptions do not exist. Also, the number of vehicles to be synchronized is unknown in advance. Therefore, in this paper we propose a method by which a vehicle can

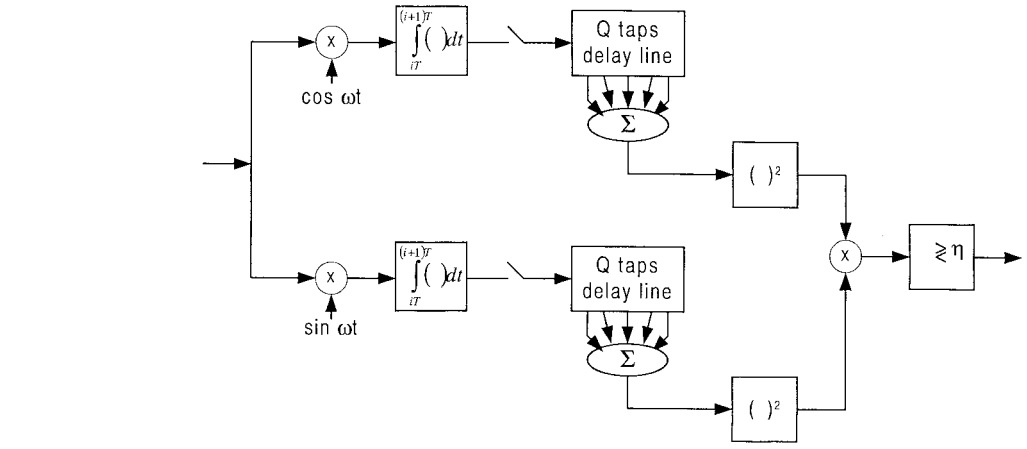


(a)

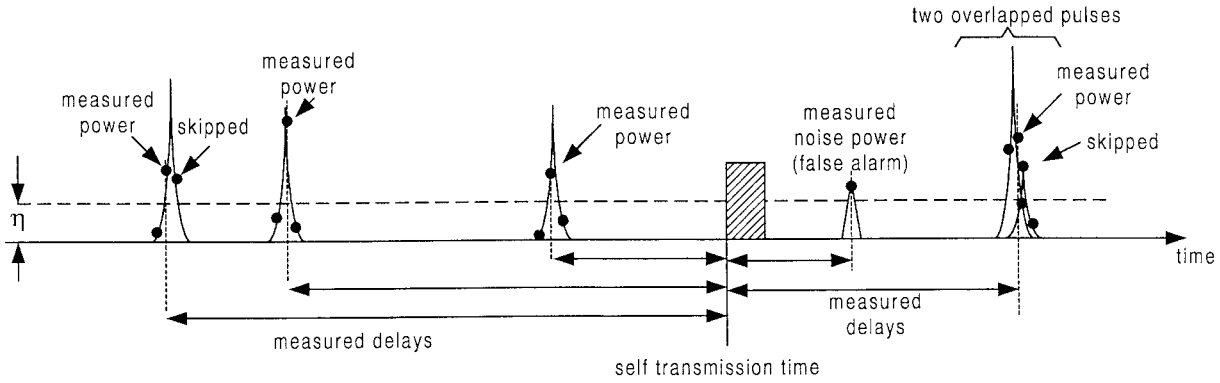


(b)

Fig. 2. (a) Square law envelope detector ($T = Tc/Q$). (b) Typical output of squared law envelope detector.

measure the power and relative delay of other vehicles, to apply Akaiwa's formula. The method does not provide a mean for propagation delay measurement. However, in intervehicle communication environment, which normally has short distances among communicating vehicles, this propagation delay is negligible w.r.t. the period of the synchronization signal. This was confirmed in our computer simulation. Moreover, this drift is not a major deficiency in intervehicle communication since there is no wire-line clock interface problem. When clocks of all communicating vehicles drift slowly, in the same direction, they can still communicate since slot timing is the same and there is sufficient guard time. At any case, the effect of drift is an issue that is to be dealt with in the communication part of the system design.

The proposed method is as follows. Each vehicle transmits a periodic pulse train of period $GT_c$ where $T_c$ is the pulse duration. The proposed carrier frequency is in the 60-GHz band [7]. Propagation characteristics, including weather effects, for this band are found in [22]. Similar to packet data communication systems, the same carrier frequency is used by all vehicles. The purpose of the synchronization system is to eventually make all vehicles transmit their periodic pulses simultaneously to mark the start of packet data slots. However, before synchronization is completed, the durations among pulse trains are not equal. All vehicles continuously monitor the channel. We define a *monitoring period* for each pulse a vehicle transmits. The monitoring period starts from $0.5GT_c$ before the positive edge of the pulse to $0.5GT_c$ after the positive edge. During the monitoring period a vehicle measures the power and relative delay (w.r.t. its own positive edge) for all detectable pulses. However, a vehicle turns off its receiver during transmitting its own pulse. Note that if two vehicles are synchronized they do not *feel* the existence of each other. The detection process is explained in more details in Section IV. At the end of the monitoring period each vehicle decides the time of transmitting its next pulse according to

$$t_i|\text{new} = t_i|\text{old} + GT_c + \alpha \frac{\sum_{\text{pulses}\geq\eta} t_{k,i} P_{k,i}}{\sum_{\text{pulses}\geq\eta} P_{k,i}} \tag{1}$$

where $t_i|$old and $t_i|$new are absolute transmission time, w.r.t. a zero time origin, They correspond to the positive edges of two successive pulses from vehicle $i$, respectively. The parameter $\alpha$ ($\alpha \leq 1$) decides the speed of convergence. In this paper, we take $\alpha = 0.5$. The power of the pulse of vehicle $k$, measured by vehicle $i$, is denoted as $P_{k,i}$. Also, $t_{k,i}$ is the time difference (positive or negative) between the positive edges of the pulses from vehicles $k$ and $i$, with vehicle $i$ taken as reference. The method for measuring $P_{k,i}$ and $t_{k,i}$ is given

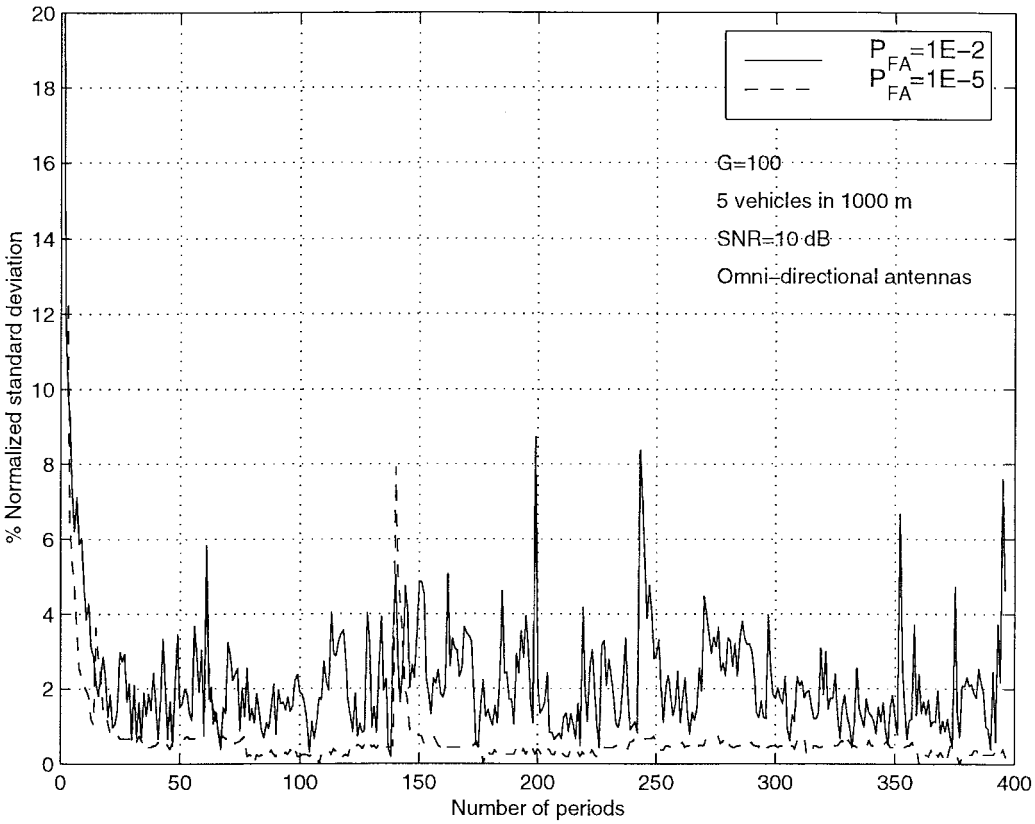


Fig. 3. Effect of $P_{FA}$ in one realization of the synchronization process.

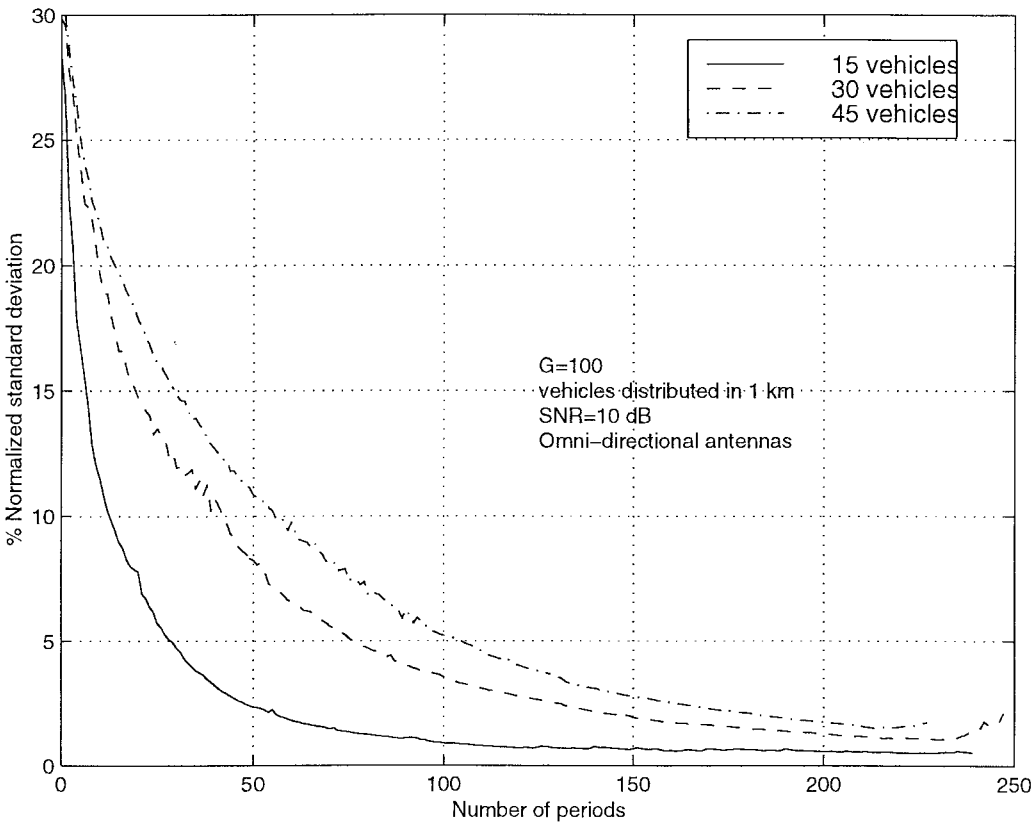


Fig. 4. Effect of number of vehicles on the speed of synchronization.

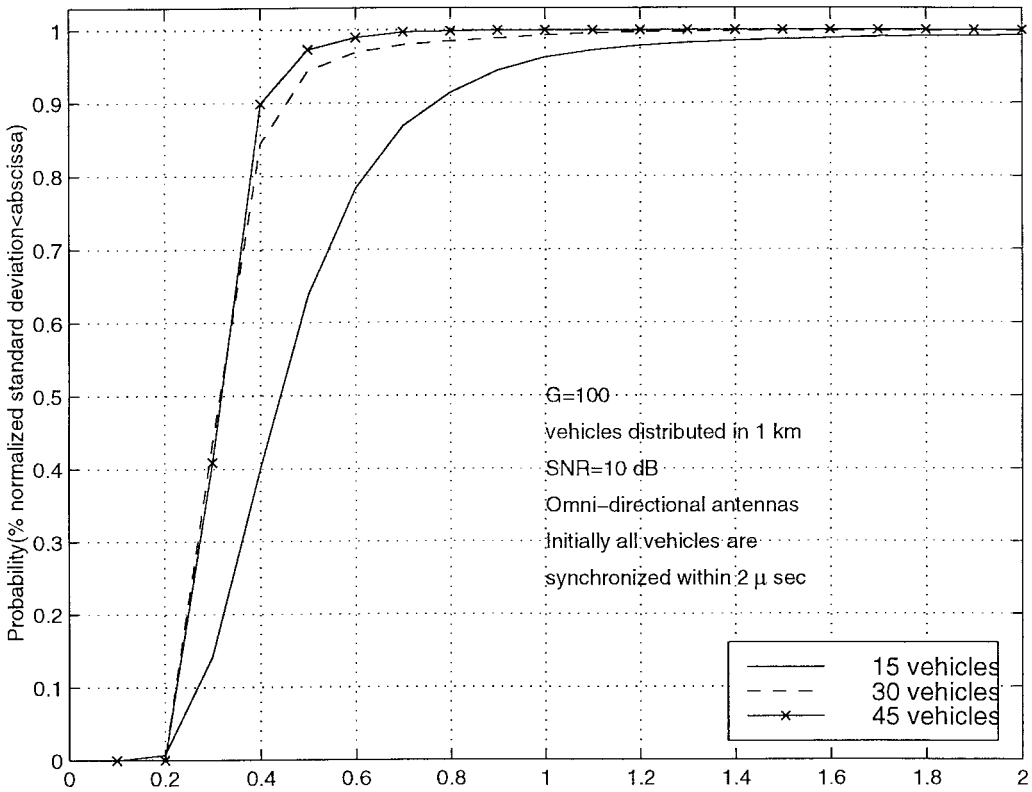


Fig. 5. Cumulative distribution function of % normalized standard deviation.

in Section IV. Note that if all vehicles become synchronous, they cannot measure each other. In this case, the last term in the right-hand side (r.h.s.) of (1) is small, since $P_{k,i}$ becomes due to noise only. In this case, all pulse trains continue to be approximately periodic, with period $GT_c$. Fig. 1 shows an example for four vehicles, and vehicle 2 is applying (1). In Fig. 1, *scheduled transmission* denotes the pulse that would have been transmitted if the period was not adjusted.

It is important to make the following notes.

1) Each vehicle simply measures power and delay of those pulses that fall in the monitoring period of pulse "old" to decide the time to send pulse "new." The identity of the vehicles producing the measured pulses is unknown.
2) Synchronous vehicles cannot measure the pulses of each other. Because of that, if $\alpha = 1$, some initial conditions may lead to a situation where vehicles in close vicinity get divided into two groups, each in a synchronous state within itself. The two groups never get synchronized together. The same observation is noted in [2] if the cellular system consists of two base stations only. Hence, $\alpha$ should not be set close to one.
3) Some vehicles may not be included in the summation in the r.h.s. of (1). This is because either the pulse power is lower than a threshold $\eta$, or it does not lie in the monitoring period. The latter case occurs at the beginning of the process if a vehicle gets a large positive value for the third term in the r.h.s. of (1) which makes its interpulse duration $\gg GT_c$, which makes it go out of the monitoring period if another vehicle. On the other hand, in many cases a vehicle is included twice in monitoring period if another vehicle if the above-mentioned term is a large negative.
4) Although the propagation delay considered in [1] and [2] is not included in (1), yet for intervehicle environment system parameters we find that after convergence the third term in the r.h.s. of (1) is very close to zero for all vehicles and no clock drift occurs.
5) For any value of $\alpha$, the third term in the r.h.s. of (1) is always $\geq -0.5\ GT_c$. Therefore, at the end of the monitoring period (i.e., at $t_i|\text{old} + 0.5\ GT_c$) the waiting time before new transmission is $\geq 0$ and there is no problem in applying (1).

## III. Channel Model

Most of our numerical results rely on a conventional additive white Gaussian noise (AWGN) channel. However, we also consider the effect of a simplified Rician multipath fading channel. The signal from vehicle "$k$" to vehicle $i$ consists of two parts, a line of sight (LOS) nonfaded path and a Rayleigh faded path. The power ratio of the LOS path to the faded path, as measured by vehicle $i$, is denoted as $\Gamma$, which we take as a constant in the system. The faded path is due to reflections from near objects, such as other vehicles. The received signal by vehicle $i$ from vehicle $k$ can be written as

$$r_{k,i} = n_i(t) + Ap(t - t_k - \zeta_{k,i})\sqrt{L_{k,i}}\cos(\omega t + \phi_{k,i}) + \beta R_{k,i} Ap(t - t_k - \zeta_{k,i})\sqrt{L_{k,i}}\cos(\omega t + \theta_{k,i}) \quad (2)$$

where $n_i$ the AWGN with two-sided power spectral density $N_o/2$ and is independent for all vehicles $i$. The constant $A$ is

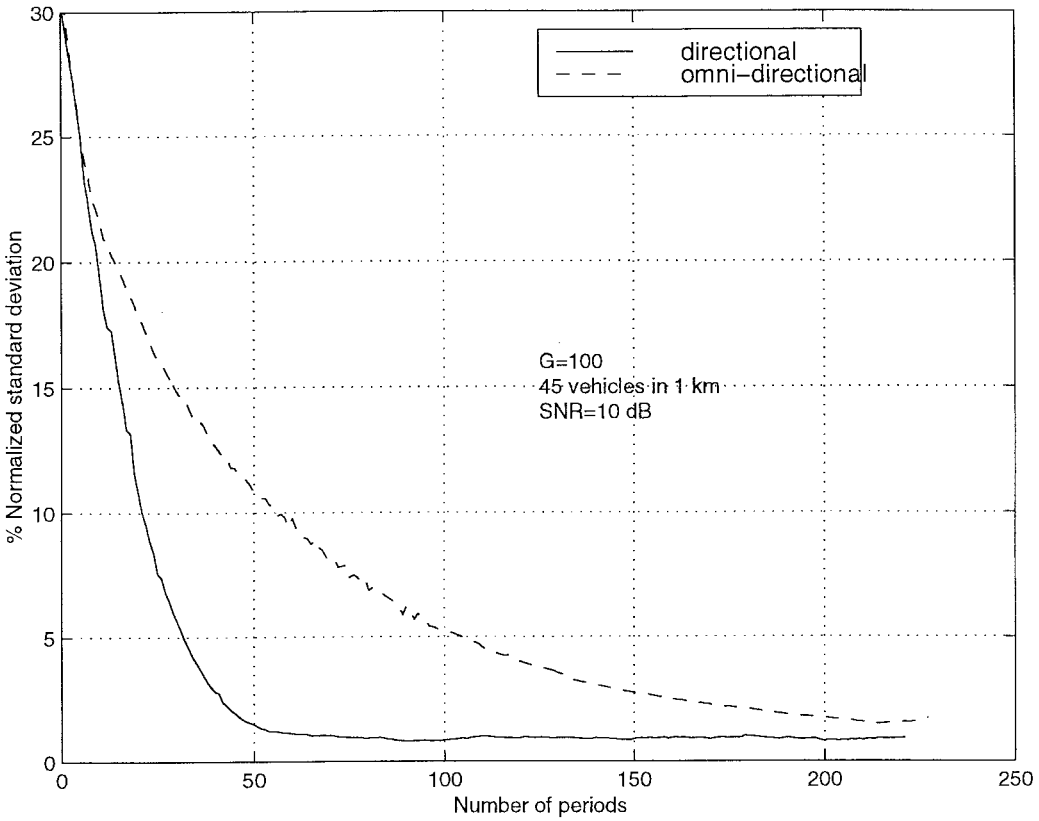


Fig. 6. Effect of antenna diversity on the speed of synchronization.

the amplitude of the pulse train $p(t)$ which has a period $GT_c$ as described in Section II. The carrier frequency is denoted by $\omega$ rad/s. The time $t_k$ is the absolute time of the positive edge of the first pulse generated by vehicle $k$. Also, $\zeta_{k,i} \equiv \zeta_{i,k}$ is the propagation delay between vehicles $i$ and $k$ and $\phi_{k,i}$ is a random phase angle uniformly distributed in $[0, 2\pi]$. $\phi_{k,i}$ is independent for all $k$ and $i$ and also independent among successive pulses. The power path loss of both the LOS and faded paths is $L_{k,i} = Z^2/d_{k,i}^{\gamma}$, where $\gamma$ is a constant, $d_{k,i}$ is the distance between vehicles $k$ and $i$ and the constant $Z$ is defined as the distance at which, if $\gamma = 2$, the path loss $L_{k,i} = 1$. The value of $\gamma$ decides the path loss. Higher $\gamma$ occurs due to oxygen absorption, water vapor, and rain in windows in the 60-GHz range [21], [22].

We turn our attention to the fading channel parameters where we assume that the channel between vehicle $i$ and $k$ is the same as between $k$ and $i$. The parameter $\beta$ decides the power ratio $\Gamma$ ($\Gamma = 1/2\beta^2$) between the LOS and faded paths. The random variables $R_{k,i} = R_{i,k}$ are independent and Rayleigh distributed with a unity parameter. $R_{k,i}$ and $R_{k',i}$ are independent for $k' \neq k$. The random phase angles $\theta_{k,i}$ are all uniform in $[0, 2\pi]$, and their interrelations are the same as the Rayleigh envelops. In our simulation, we generate a new set of random variables $R_{k,i}$ and $\theta_{k,i}$ every coherence time of $2\pi c/(\omega v)$, where $c$ is the speed of light and $v$ is the vehicle speed.

Recalling the equation for the path loss, if $\gamma = 2$ we get $L_{k,i} = 1$ at a distance $d_{k,i} = Z$. At this distance, the total average signal-to-noise ratio (SNR) vehicle produces is SNR $= (A^2 T_c/2N_o)(1 + (1/\Gamma))$. Using this equation, in this paper SNR is defined the signal to noise ratio that is generated at a distance $d_{k,i} = Z$ when $\gamma = 2$ and $L_{k,i} = 1$.

Finally, only when considering the nonfading channel, we also consider the effect of directive antennas. The LOS term of (2) is also multiplied by $G_{k,i}$ which is the product of the receiver and transmitter antenna gains, given the transmission and reception angles on the antenna gain patterns. For both the transmit and receive antennas, we use the amplitude antenna gain pattern $G(\rho) = \text{Sinc}(2.78\rho/\rho_{BW})$, where $\text{Sinc}(x) = \sin(x)/x$ and $\rho_{BW}$ is the 3-dB beam width. When considering directive antennas we assume the receiving antenna is directed to the front to receive from the front (direction of driving) and the transmitting antenna is directed to the back. Depending on vehicle locations, the appropriate angles are calculated and the antenna gains are found. We do not consider directive antennas in the simulation of fading channel since we do not know the angles of arrival and departure of the faded paths, especially when the distance between two vehicles is small.

## IV. Pulse Detection

Each vehicle uses a square law envelope detector to detect the existence of pulses and measure their power and delay. The square law envelope detector is shown in Fig. 2(a). In the in-phase and quadrature-phase branches, it includes integration over duration of $T_c/Q$, where $Q$ is an integer. We denote each output due to one integration period as a *sample*. This is equivalent to a sampling frequency of $Q/T_c$. Then, $Q$

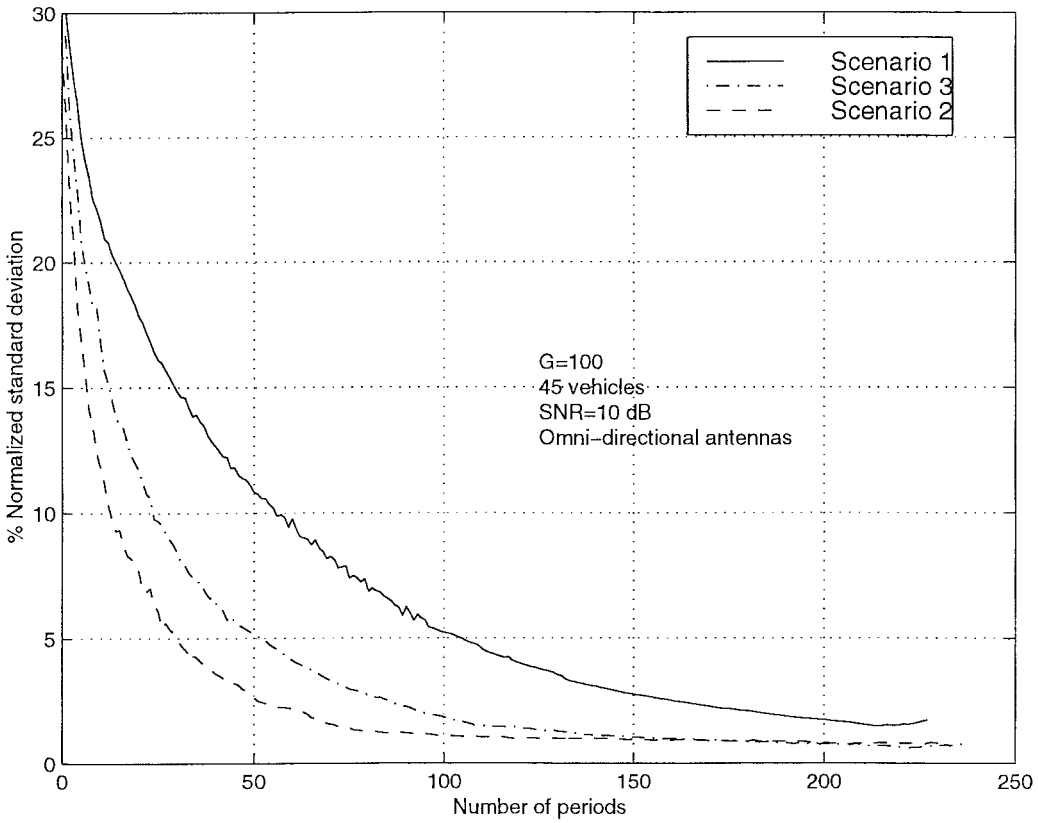


Fig. 7. Effect of traffic scenario on the speed of synchronization.

successive samples are added, squared and added to the other branch to produce one envelope detector output sample. This sample is compared to a threshold $\eta$ to decide whether a pulse exists in the previous duration of $T_c$. A typical output of the envelope detector is shown in Fig. 2(b). In simulation, we take $T_c/Q$ as the smallest time unit.

We denote the output of the in-phase and quadrature-phase integrators of vehicle $i$ due to vehicle $k$ as $r_c$ and $r_s$, respectively. Normalizing by the factor $\sqrt{N_o T_c/4Q}$, when a pulse is transmitted from vehicle $k$, and after a propagation delay $\zeta_{k,i}, Q$ samples for $r_c$ containing LOS and faded paths are generated as

$$r_c = \sqrt{\frac{2\Gamma L_{k,i}\mathrm{SNR}}{Q(1+\Gamma)}}\cos\phi_{k,i} + \sqrt{\frac{L_{k,i}\mathrm{SNR}}{Q(1+\Gamma)}}R_{k,i}\cos\theta_{k,i}. \quad (3)$$

Similarly, $r_s$ is same as (3), but with "cos" replaced by "sin." Without going into the details of the simulation algorithm we state that when vehicle $i$ transmits a pulse the simulation program decides the start time and end time of the monitoring period, as shown in Fig. 1 for the example of vehicle 2. The program then opens two arrays, each of length $GQ$, to store the in-phase and quadrature-phase samples during this monitoring period. The in-phase and quadrature-phase samples, due to all vehicles, are added at their appropriate timing according to their time of origination and propagation delay with vehicle $i$. Finally, independent zero mean Gaussian r.v's. with unit variance are added to each sample in both the in-phase and out-of-phase branches to simulate the AWGN. Note that before normalization, these noise samples had a variance of $N_o T_c/4Q$.

As shown in Fig. 2(a), the in-phase and quadrature-phase samples are applied to the two delay lines, adders, square law devices, and finally added to get the envelope detector output samples. If the envelope detector output exceeds $\eta$, a pulse is assumed to exist with power equal to the square law envelope detector output. Its delay is its time w.r.t. the transmission time of the pulse of vehicle $i$. Note that one received pulse produces $2Q-1$ samples at the output of the envelope detector. To avoid counting a pulse twice, when a sample is detected the next $2Q-2$ envelope detector output samples are skipped [even if this leads to skipping another pulse, as shown in an example in Fig. 2(b)].

False alarm occurs when the noise power exceeds $\eta$ and hence considered as a legitimate pulse. When no real pulse exists, the output of the in-phase and quadrature-phase integrators are independent Gaussian noise samples with zero mean and unit variance. Adding $Q$ successive samples produce a $\chi^2$ distributed envelope detector output sample [20]. The probability of false alarm is given by

$$P_{FA} = \exp(-\eta/2Q). \quad (4)$$

The threshold $\eta$ is selected to guarantee an acceptable probability of false alarm. Without fading the envelope detector output of vehicle $i$ due to vehicle $k$ is give by $2QL_{k,i}\mathrm{SNR}$.

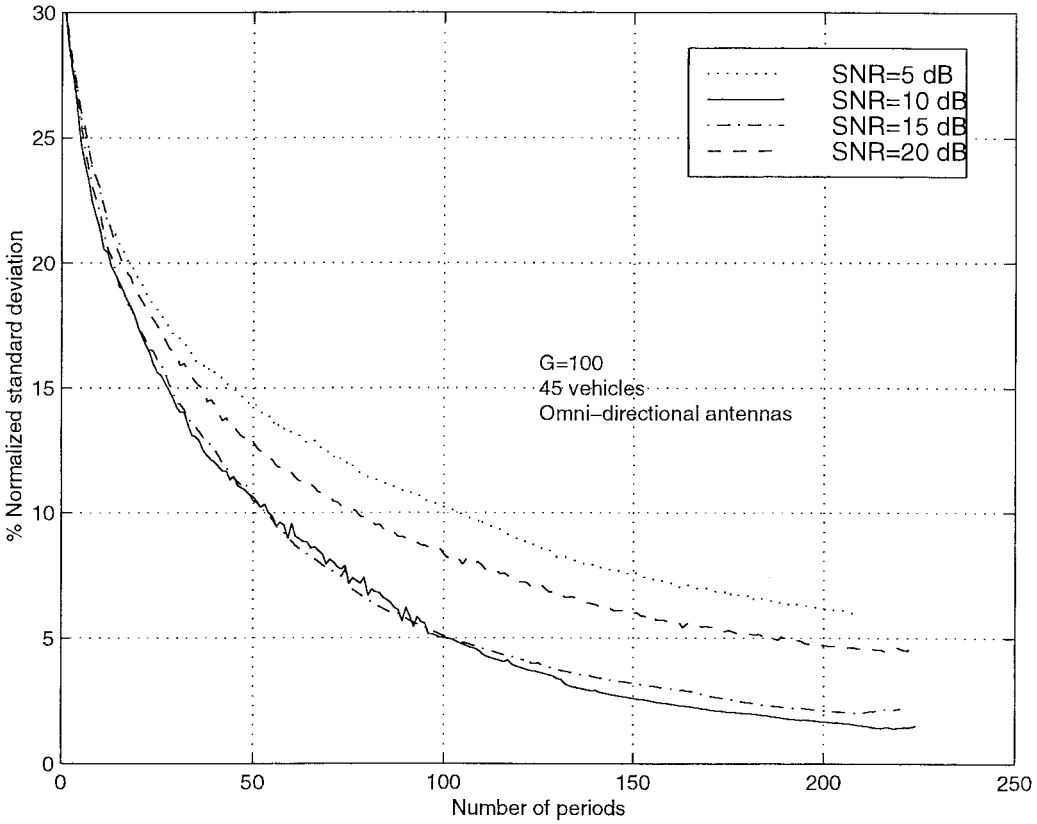


Fig. 8. Effect of SNR on the speed of synchronization.

For this envelope to exceed $\eta$ the distance must be

$$d_{k,i} \leq \left( \frac{Z^2 \text{SNR}}{-\ln\ P_{FA}} \right)^{1/\gamma}. \tag{5}$$

Hence, for synchronization to start we need at least two vehicles with headway following (5). Once these two vehicles are synchronized and if the propagation delay between them is smaller than $T_c$, their pulses coincide in time and add (though not in phase). Their power can then reach further distance and more vehicles get synchronized with them. For example, if each vehicle produces SNR $=$ 10 dB at $Z = 300$ m, and if $P_{FA} = 1E-5$ and $\gamma = 2$, then (5) results in 280 m. Vehicles within LOS and at a much smaller headway are usually available.

## V. Simulation Procedures

We simulate the system with three traffic scenarios. In all cases the speed of any vehicle is an independent Gaussian r.v. with mean 80 km/h and standard deviation 5 km/h. Uniform distribution with mean 80 km/h and standard deviation of 5 km/h is also attempted, but it did not make a significant difference. The results reported in this paper are for the Gaussian distribution. The traffic scenarios are as follows.

1) This is our benchmark scenario. $K$ vehicles are initially distributed randomly, via a uniform probability density function, over 1 km of a one-lane road.
2) Vehicles are in three groups driving on one lane. Group $j$ has $K/3$ vehicles, distributed randomly over a distance from $j$ to $j + 0.3$ km, $j = 0, 1, 2$.
3) Vehicles are in two groups driving on two lanes in the same direction. Group $j$ on lane $j$ has $K/2$ vehicles distributed randomly from $j$ to $j + 0.3$ km, $j = 0, 1$. The distance between the two lanes is 4 m.

In all cases a vehicle is represented by a point with certain coordinates. However, we force the distance between any vehicles to be at least 1 m. Motion is updated every 0.03 s with a new speed assigned to each vehicle and, hence, new coordinates calculated (66-cm movement on the average). In all cases, synchronization is completed before vehicles make any significant movement. However, vehicle speed affects coherence time in fading channels, which is calculated using 80 km/h. Also, the three scenarios provide possible grouping situations on the road. The simulation program proceeds as follows.

1) Vehicles are distributed according to the selected scenario. Distances, propagation delays, path losses, angles, and antenna gains among all vehicles are calculated. All are updated every 0.03 s.
2) A set of Rayleigh gains and random phases is generated with the characteristics described earlier. A new set is generated every coherence time.
3) Each vehicle transmits the first pulse at a random time in $[0, GT_c)$.

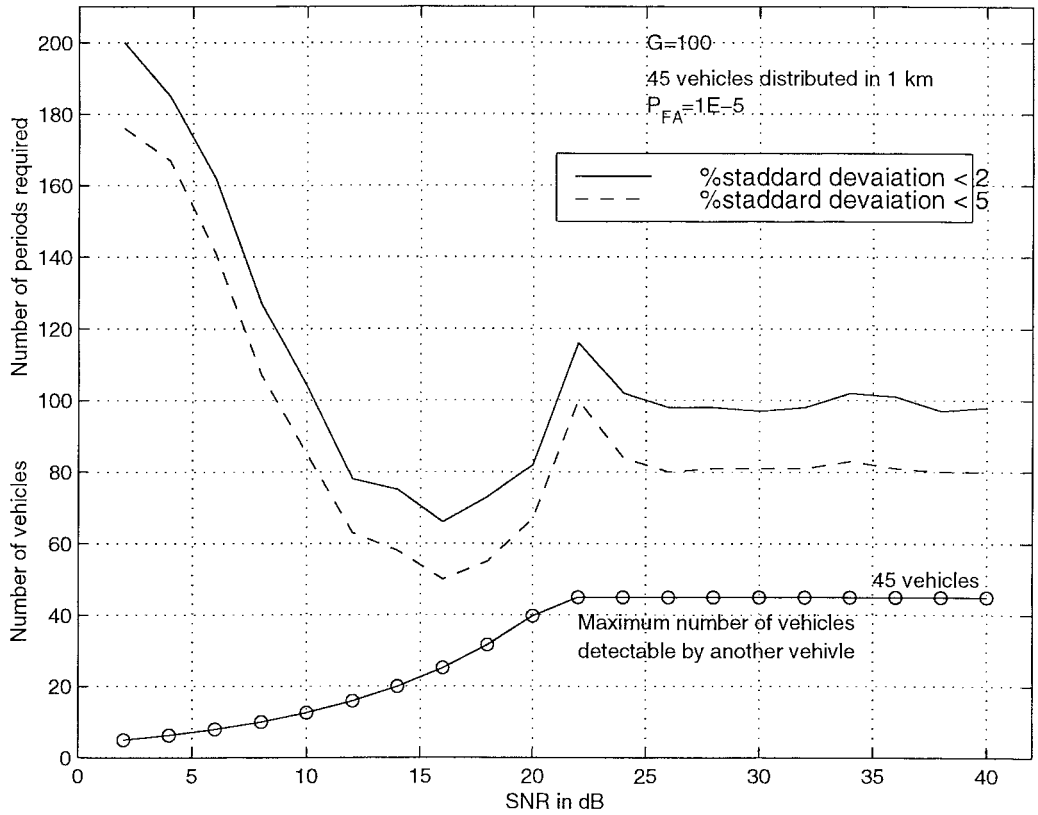


Fig. 9. Effect of SNR on the speed of synchronization on an ideal system.

4) Vehicles are considered in an ascending order according to the ending time of their monitoring periods (decision time for vehicle 2 in Fig. 1). The program considers each vehicle in turn (see note below). At its turn, the program calculates the envelope detector output for the whole monitoring period of that vehicle, finds power and delay of detected pulses, applies (1) to find its new pulse time and its new monitoring period. The older pulse transmission time is kept in memory to be used for other vehicles. Vehicles are time resorted if needed depending on the newly generated transmission time and decision time.
5) Step 4) is repeated until convergence.

It is worth mentioning that many other traffic scenarios could occur. The above scenarios are just examples which can used to predict performance in other scenarios. For example, if two groups of synchronized vehicles meet, the initial conditions will be simpler since there are already vehicles that are synchronized. In this case, synchronization will be temporarily lost until resynchronization occurs.

## VI. Numerical Results and Discussions

The performance measure used for system evaluation is the normalized standard deviation. For each iteration, after updating $t_i|$new for all vehicles in the system we calculate the normalized mean time

$$\bar{t} = \frac{1}{KGT_c} \sum_{k=1}^{k} t_k|\text{old}. \tag{6}$$

This is approximately the number of periods that has passed till this time and is used in the abscissa of most figures. The normalized standard deviation is given by

$$\sigma_t = \frac{1}{GT_c} \sqrt{\frac{1}{K} \sum_{k=1}^{K} t_k|\text{old} - \left( \frac{1}{K} \sum_{k=1}^{k} t_k|\text{old} \right)^2}. \tag{7}$$

Small standard deviation indicates that pulses are more tightly synchronized. For scenarios 2 and 3, we do not use the total number of vehicles $K$ in (6) and (7) but only the vehicles in group $j = 1$, i.e., data is collected from group $j = 1$ only. This is because the important objective is to have each group synchronized within itself. Communication with another group, more than 1 km away, is not important. However, it is interesting to note that when a group is synchronized and the transmitted pulses become almost simultaneous, the signal from one group crosses the 1-km gap and reaches the other group and all system is synchronized.

Unless otherwise mentioned, we use the following default settings: $Q = 2$ samples/pulse, $G = 100$ pulses/period, pulse duration $T_c = 1$ $\mu$s, path-loss exponent $\gamma = 2$, $P_{FA} = 1E-5$, and SNR $= 10$ dB at $Z = 300$ m, omnidirectional antennas, nonfading channel, and the first traffic scenario. When directive antennas are used, the beam width $\rho_{BW} = 20°$.

Fig. 3 shows the effect $P_{FA}$ in one realization of the first scenario with $K = 5$ vehicles. We recall that when all signals

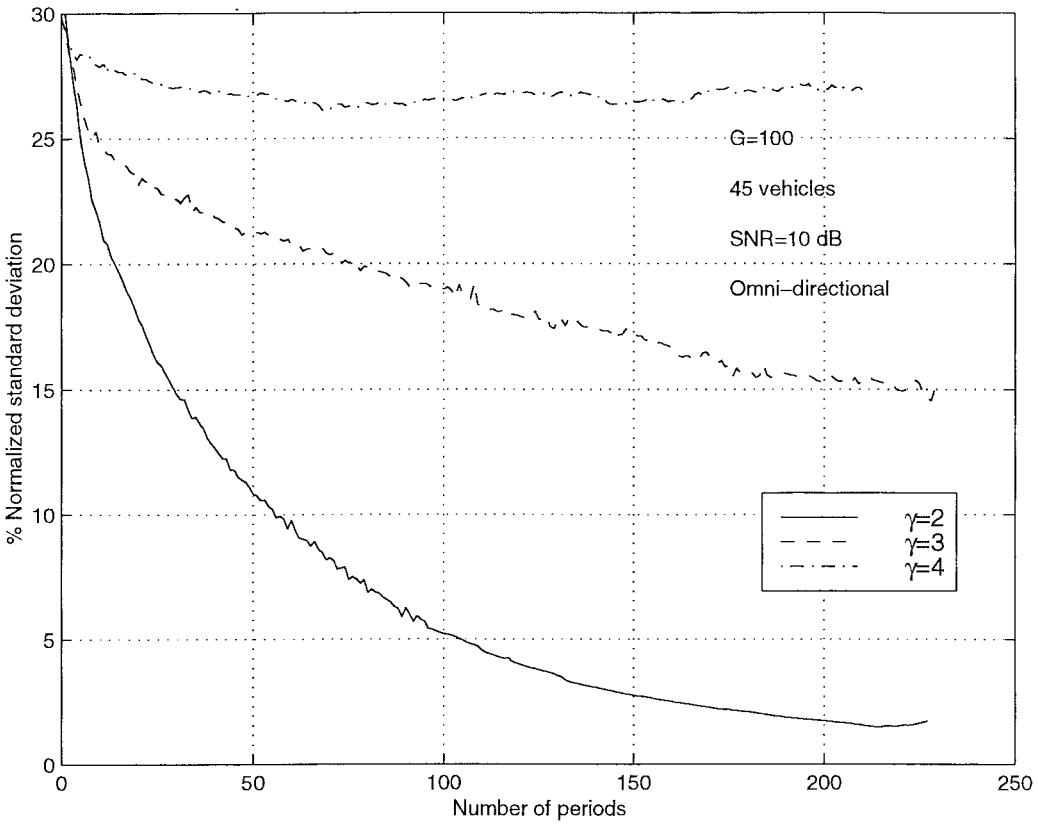


Fig. 10. Effect of path-loss exponent on the speed of synchronization.

are synchronized vehicles cannot measure each other. The effect of this point can be seen in Fig. 3. In Fig. 3, when the normalized standard deviation touches zero (i.e., all vehicles exactly synchronized), if a vehicle detects a noise pulse, it assumes it is a vehicle legitimate transmitted pulse. In this case, this will be the only pulse it can measure and the vehicle will apply (1) to try to synchronize with it. However, once it is out of synchronization it can measure all other vehicles strongly added power, and in the next pulse period it is back to synchronization. This explains the spikes in the plot after the normalized standard deviation goes to zero. This also signifies the importance of low $P_{FA}$. Although not shown here, when the number of vehicles is larger the curve is smoother.

For the remaining numerical results the synchronization process is repeated all over for 150 times. New random initial pulse transmission times are generated for all vehicles and new random initial locations in the traffic scenario are given. The 150 results are averaged. Using 300 instead of 150 did not make a considerable difference.

Fig. 4 shows the effect of the number of vehicles. As expected for a larger number of vehicles synchronization is slower. However, it is always completed in a reasonable time (200 periods $=$ 20 ms). We note that the effect of vehicles speed is found to be insignificant. As shown in Fig. 4, and the subsequent results, synchronization is completed before the vehicles make any significant motion.

In Fig. 5, we start the system with an approximately synchronized state. The initial transmission time of each vehicle is a r.v. uniformly distributed in [0,0.02 $GT_c$). The synchronization process is started and continued for 250 periods and cumulative distribution for the standard deviation is calculated. Since we assume the synchronization system is continuously running in parallel to data transmission (but on a different frequency) Fig. 5 shows the performance of the system as it continues after synchronization is achieved. To the contrary of Fig. 4, the higher number of vehicles provides a more stable synchronization. In all shown cases, the normalized standard deviation is less than 4%. Fig. 5 is repeated with starting r.v.'s in [0, 0.05 $GT_c$) and no significant difference is found.

Fig. 6 studies the performance with directive antennas in scenario 1 with 45 vehicles. It is found that directive antennas (both transmit and receive antennas are directive) provides faster synchronization. In this case, each vehicle synchronizes with (receives from) the ones in front of it. Directive antennas make synchronization some where between a complete decentralized synchronization with all vehicles are at equal footing (omnidirectional antennas), and a complete centralized synchronization with all vehicles synchronizing to one source.

Fig. 7 studies the effect of traffic scenarios 1–3 with omnidirectional antennas with $K = 45$ ($K = 46$ in scenario 3). In scenarios 2 and 3, data is collected only from the group $j = 1$ as mentioned earlier. However, all $K$ vehicles interact. It is found that scenario 2, with the smallest number of vehicles per group, synchronizes the fastest. Although not shown here, it is found that in scenarios 2 and 3 all vehicles in all groups get synchronized.

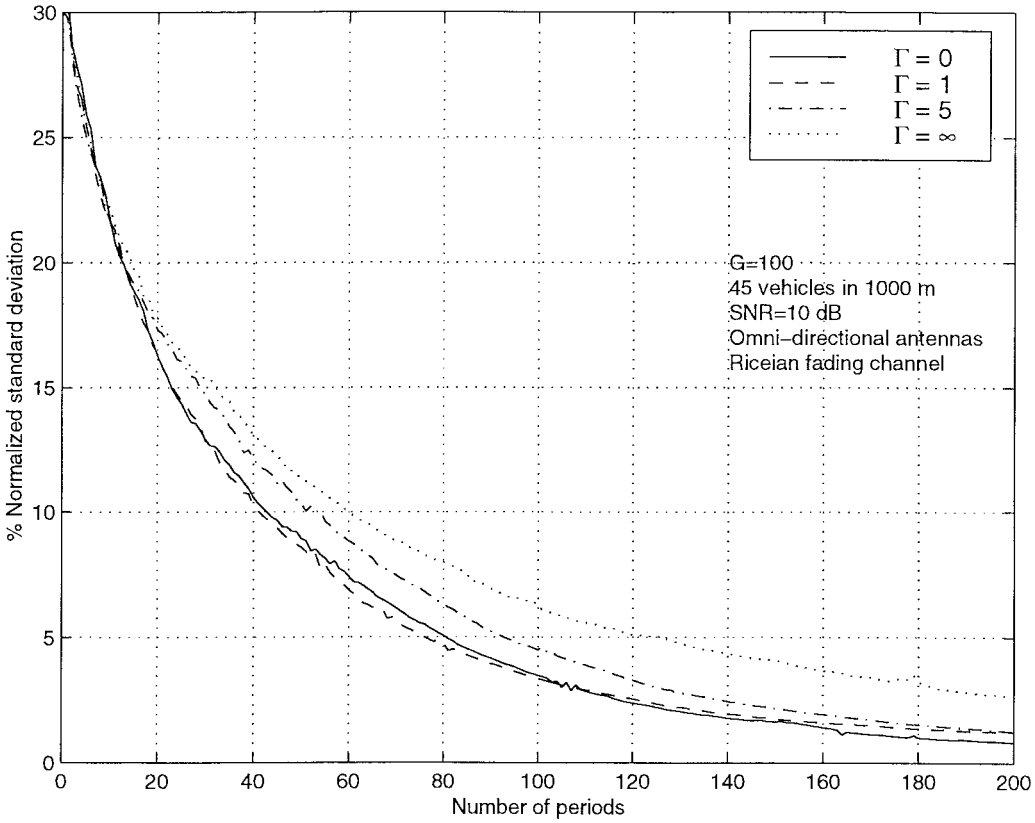


Fig. 11. Effect of fading channel on the speed of synchronization.

Fig. 8 shows the effect of SNR on the speed of synchronization. From Fig. 8, we note that the performance is nonlinear with SNR. SNR $= 10$ dB provides faster synchronization than 5 and 20 dB. To explain this behavior, we recall that increasing the signal power has two effects.

1) The system is less noisy, which obviously improves the synchronization speed.
2) A larger number of vehicles, located at further distances, detect each other. Hence, the process is initiated with a larger population. This may reduce the synchronization speed.

This leads us to assume that, given a certain traffic scenario, there is an optimum value of SNR. To confirm the existence of this tradeoff we make a simulation experiment, which is reported below.

To test the tradeoff mentioned above we study a hypothetical idealized scenario. We simulate a system with 45 vehicles fixed at equal intervals, over a 1-km line. Vehicles are not allowed to move. Their initial pulse transmission time is also distributed with equal time intervals over $GT_c$. AWGN is removed. This makes a deterministic system without any random component, except for the phase angles in (2). We vary the SNR parameter in (3) (in this case SNR is a normalized transmitted power) and for each value we find the number of periods required for the system to reach a 5% and 2% normalized standard deviation. Also, for each value of SNR (i.e., normalized transmitted power) we find the number of vehicles covered by the distance given by (5). This number is the maximum number of vehicles whose pulse power can be another vehicle by exceeding the threshold $\eta$. The results are shown in Fig. 9. We can observe that an optimum SNR value of 16 dB exists (i.e., normalized power exists). This value causes the maximum number of vehicles detectable by other vehicle to be $K/2$. Although we cannot generalize this value, however, we confirm that an optimum value of SNR exists and the performance is a nonmonotonic function of SNR.

Fig. 10 shows the effect of the path-loss exponent $\gamma$. When $\gamma$ is increased to three the performance deteriorates very severely. At $\gamma = 4$, no synchronization is achieved. Note that the distance given by (5) reduces from 279 to 43 and then 16 m when $\gamma$ is increased. Higher SNR is needed to achieve synchronization in this case.

We now turn our attention to the fading channel. The general effect of the number of vehicles, directional antennas, traffic scenarios, and path-loss exponent is similar to the nonfading case, and there is no need to show new results. Fig. 11 shows the effect of different values of $\Gamma$ on the speed of synchronization. Interestingly, it is found that synchronization is faster for smaller $\Gamma$ (weaker LOS component). Although the difference is not large, but this is an unexpected observation. One possible explanation is that the fading channel slightly reduces the number of vehicles that start synchronization together.

Fig. 12 is similar to Fig. 5, but for the fading channel. Moreover, we vary the parameter $\Gamma$ instead of the number of vehicles. It is shown that, after initial synchronization

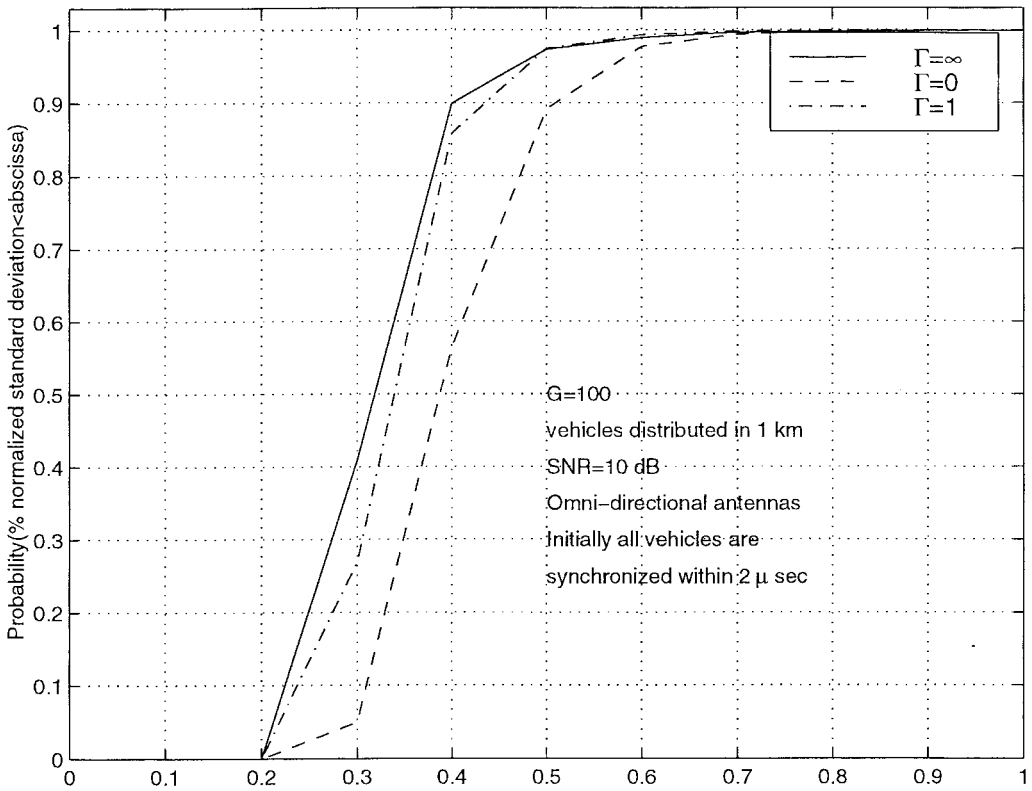


Fig. 12. Cumulative distribution function of % normalized standard deviation in fading channel.

has taken place, the nonfading channel keeps a more stable synchronization. Although we have not done an exhaustive search over all parameters, but we generally observe that in both nonfading and fading channels when synchronization is faster it is less stable. However, in all tried parameters synchronization speed and stability were satisfactory.

## VII. Conclusions

Vehicle-to-vehicle communication is an important part of the IVHS. For data exchange among vehicles, synchronization is required. We present a system to achieve this synchronization. Each vehicle transmits a periodic train of pulses. Using these pules each vehicle can measure the delay of other vehicles signals with respect to its own signal and hence adjusts its own delay. Eventually all vehicles are synchronized. The proposed system is studied in a nonfading and fading channels. With the parameters used in the paper it is found that synchronization is achieved in less then 20 ms with vehicle density up to 45 per km and pulse train period of 100 $\mu$s. After synchronization is achieved, the normalized standard deviation stays below 3% for 99% of the time. The use of directive antennas speeds up the synchronization process. Higher power does not necessarily improve the speed of synchronization, but if the path loss is high due to oxygen absorption, fog, or rain high power is needed. The system performs satisfactorily in fading channels.

## References

[1] Y. Akaiwa, H. Andoh, and T. Kohama, "Autonomous decentralized inter-base station synchronization for TDMA microcellular systems," in *IEEE Veh. Technol. Conf.*, May 1991, pp. 257–262.

[2] J. Chuang, "Autonomous time synchronization among radio ports in wireless personal communication," *IEEE Trans. Veh. Technol.*, vol. 43, pp. 27–32, Feb. 1994.

[3] A. Hirukawa and H. Takanashi, "Inter-base station TDMA frame synchronization technique for street microcellular systems," in *Proc. Personal, Indoor and Mobile Radio Communication Conf., PIMRC'94*, The Hague, The Netherlands, Sept. 18–22, 1994, pp. 358–362.

[4] J.-M. Valade, "Vehicle to vehicle communications: Experimental results and implementation perspectives," in *2nd World Congress on Intelligent Transport Syst. '95*, Yokohama, Japan, Nov. 9–11, 1995, pp. 1606–1613.

[5] H. Akazawa and M. Nakagawa, "Autonomous decentralized synchronization system for the inter-vehicle communication network," in *Proc. 2nd World Congress on Intelligent Transport Syst. '95*, Yokohama, Japan, Nov. 9–11, 1995, pp. 1594–1599.

[6] D. Hubner and S. Hoff, "Simulative evaluation of a decentralized packet synchronization algorithm for short range mobile radio networks," in *Proc. Globecom '95*, pp. 1349–1353.

[7] W. Kremer, D. Hubner, S. Holf, T. Benz, and W. Schafer, "Computer aided design and evaluation of mobile radio local area networks in RTI/IVHS environments," *IEEE J. Select. Areas Commun.*, vol. 11, Apr. 1993.

[8] S. Tabbane and P. Godlewski, "Performance evaluation of the R-BTMA protocol in a distributed mobile radio network context," *IEEE Trans. Veh. Technol.*, vol. 41, Feb. 1992.

[9] H. Fujii, K. Seki, and N. Nakagata, "Experimental research on protocol of inter-vehicle communication for vehicle control and driver support," in *2nd World Congress on Intelligent Transport Syst. '95*, Yokohama, Japan, Nov. 9–11, 1995, pp. 1600–1605.

[10] T. Hatakeyama and S. Takaba, "A network architecture of the inter-vehicle packet communication system," in *IEEE Vehicle Navigation and Information Syst. Conf. '94*, Yokohama, Japan, Aug. 31–Sept. 2, 1994, pp. 159–164.

[11] K. Mizui, M. Uchida, and M. Nakagawa, "Vehicle to vehicle communication and ranging system using spread spectrum technique—Proposal

of double boomerang transmission system," in *IEEE Vehicle Navigation and Information Syst. Conf. '94*, Yokohama, Japan, Aug. 31–Sept. 2, 1994, pp. 153–158.
[12] I. Sasaki, T. Hirayama, and T. Hatsuda, "Vehicle information network based on inter-vehicle communication by laser beam injection and retro-reflection techniques," in *IEEE Vehicle Navigation and Information Syst. Conf. '94*, Yokohama, Japan, Aug. 31–Sept. 2, 1994, pp. 165–169.
[13] R. Hager, M. Rudolf, and J. Mattfeldt, "Intelligent cruise control and reliable communication of mobile stations," *IEEE Trans. Veh. Technol.*, vol. 44, pp. 443–448, Aug. 1995.
[14] S. Shladover, C. Desoer, J. C. Rick, M. Tokmizuka, J. Walrand, W.-B. Zhang, D. McMahon, H. Peng, S. Sheikholeslam, and N. McJeown, "Automatic vehicle control developments in the PATH program," *IEEE Trans. Veh. Technol.*, vol. 40, pp. 114–130, Feb. 1991.
[15] Y. Inoue and M. Nakagawa, "MAC protocol for inter-vehicle communication network using spread spectrum technique," in *IEEE Vehicle Navigation and Information Syst. Conf. '94*, Yokohama, Japan, Aug. 31–Sept. 2, 1994, pp. 149–152.
[16] J. Kaltwasser and J. Kassubek, "A cooperative optimized channel access for inter-vehicle communication," in *IEEE Vehicle Navigation and Information Syst. Conf. '94*, Yokohama, Japan, Aug. 31–Sept. 2, 1994, pp. 145–148.
[17] A. Polydoros, A. Anastasopoulos, T.-K. Liu, P. Oannaiotou, and C. Sun, "An integrated physical/link-access layer model of packet radio architectures," California PATH Research Rep. UCB-ITS-PRR-94-20, Oct. 1994.
[18] S. Sachs and P. Varaiya, "A communication system for the control of automated vehicles," California PATH Research Rep. TECH MENFDMO-93-05, Sept. 1993.
[19] S. Streisand and J. Walrand, "A communication architecture for IVHS," California PATH Research Rep. UVB-ITS-PRR-92-10, 1992.
[20] J. Proakis, *Digital Communications*, 3rd ed. New York: McGraw-Hill, 1995.
[21] E. N. Barnhart, "Millimeter wave communications: Air-to-air application," in *Proc. SPIE, The Int. Soc. Optical Engineering*, vol. 79, May 1987, pp. 94–98.
[22] K. Allen, "A model of millimeter-wave propagation for personal communication networks in urban settings," U.S. Dept. Commerce, NTIA Rep. 91-275, Apr. 1991.

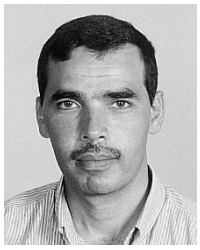

**Essam Sourour** received the B.Sc. (with honors) and M.Sc. degrees from Alexandria University, Alexandria, Egypt, in 1982 and 1986, respectively, and the Ph.D. degree from Southern Methodist University, Dallas, TX, in 1990, all in electrical engineering.

He was a Teaching Assistant at Alexandria University from 1984 to 1986 and at Southern Methodist University from 1987 to 1989. He was a System Engineer at Bell Northern Research (currently Nortel), Richardson, TX, from 1990 to 1991. He was an Assistant Professor at Alexandria University from 1992 to 1996. During 1994 and for three months in 1996, he was a Visiting Researcher at Keio University, Yokohama, Japan. Since June 1996, he has been a Senior Consultant Engineer at Ericsson, Inc., Research Triangle Park, NC. His research interests include mobile communications and spread-spectrum systems. He is currently working on projects to develop CDMA cellular phones for the third generation of cellular communication systems.

**Masao Nakagawa** (M'81) was born in Tokyo, Japan, on November 19, 1946. He received the B.E., M.E., and Ph.D. degrees from Keio University, Yokohama, Japan, all in electrical engineering, in 1969, 1971, and 1974, respectively.

Since 1973, he has been with the Department of the Electrical Engineering, Keio University, where he is now a Professor. His research interests are in spread-spectrum communication, consumer communication, mobile communication, digital broadcasting, and wireless home link. He is an Area Editor of *Wireless Personal Communications*.

Dr. Nakagawa received the IEEE Consumer Electronics Society Chester Sall Award in 1990. He was the Executive Committee Chairman of the "International Symposium on Spread Spectrum Techniques and Applications" held in Yokohama in 1992, the Program Chaiman of the "International Symposium on Information Theory and Its Applications" held in Sydney, Australia, in 1994, and one of the Guest Editors of the Special Issues on Code Division Multiple Access Networks I and II in 1994 as well as III and IV in 1996 of the IEEE JOURNAL ON SELECTED AREAS IN COMMUNICATIONS. He was the Chairman of the Study Group of Spread Spectrum Technology of the Institute of Electronics Information and Communication Engineers.